



Full Text View

[Volume 30, Issue 2 \(February 2000\)](#)

Journal of Physical Oceanography

Article: pp. 338–351 | [Abstract](#) | [PDF \(275K\)](#)

The Role of a Finite Density Jump at the Bottom of the Quasi-Continuous Ventilated Thermocline

P. Lionello*Department of Physics, University of Padua, Padua, Italy***J. Pedlosky***Woods Hole Oceanographic Institution, Woods Hole, Massachusetts*

(Manuscript received June 3, 1998, in final form March 29, 1999)

DOI: 10.1175/1520-0485(2000)030<0338:TROAFD>2.0.CO;2

ABSTRACT

The ocean thermocline is resolved in a very large number of layers by means of a recursive relation that extends the LPS model of the ventilated flow from a small to an arbitrary number of layers. In order to have simplified dynamics, the basin is semi-infinite in the zonal direction, the thermocline is fully ventilated, and its thickness vanishes at the northern boundary. In this model, the potential vorticity of each layer is shown to be inversely proportional to the Bernoulli function. The high vertical resolution adopted for the thermocline allows the study of the dependence of its motion on the ratio between the density contrast at the sea surface and the density step separating the thermocline bottom from the underlying quiescent abyss. This ratio controls both the nonlinearity and the baroclinicity of the solution. The behavior of the solution as this ratio varies from zero (linear and barotropic case) to infinity (“fully nonlinear” and baroclinic case) is described. The singularity that is found in the fully nonlinear case is discussed.

1. Introduction

The fluid motion in the ocean thermocline is a key element of the general ocean circulation and of the meridional heat transport on the planetary scale. For instance, in the midlatitude and subtropical Atlantic, the meridional Sverdrup volume transport in the thermocline, approximately 30 Sv ([Schmitz et al. 1992](#)), is much

larger than abyssal transport due to the dense water formation in the subpolar ocean, approximately 13–14 Sv (Sv $\equiv 10^6$

Table of Contents:

- [Introduction](#)
- [Model with arbitrary](#)
- [The analysis of the motion](#)
- [Conclusions](#)
- [REFERENCES](#)
- [FIGURES](#)

Options:

- [Create Reference](#)
- [Email this Article](#)
- [Add to MyArchive](#)
- [Search AMS Glossary](#)

Search CrossRef for:

- [Articles Citing This Article](#)

Search Google Scholar for:

- [P. Lionello](#)
- [J. Pedlosky](#)

$\text{m}^3 \text{s}^{-1}$) (McCartney and Talley 1984), and the thermocline meridional heat transport, approximately estimated 0.3 PW or larger, is a major share of the total transport of approximately 0.5 PW (Semtner and Chervin 1988). While the total mass transport in the thermocline determined by the Sverdrup balance, that is, forced by the curl of the wind stress, is independent on the vertical structure of the thermocline circulation, the heat transport does depend on the vertical profile of the meridional velocity. In fact, the deep layers transport water that has been subducted in the northern part of the ocean gyre and is, therefore, cooler than the water in the surface layers. The water density in the thermocline is determined by the air–sea interaction processes that modify, at the midlatitudes and in the Tropics, the temperature and salinity of the surface fluid that is subsequently subducted in the ocean interior. The density of the underlying abyss is determined by the dense water formation processes in the subpolar ocean. Therefore there is a difference in density between the thermocline and the abyss due to the different surface density in the regions where the water masses are formed. This study analyses the role of the density difference, between thermocline and abyss on the vertical structure and on the thickness of the ventilated thermocline. Precisely, this study investigates the effect of a finite density jump at the bottom of the thermocline. The density of the fluid in the thermocline is kept fixed, while the density of the quiescent abyss is allowed to change, accounting for modification of intensity of the dense water formation in the subpolar ocean.

The idea is to extend the existing multilayer LPS model of the ventilated thermocline (Luyten et al. 1983) to an arbitrary number of layers and to let their number become very large. In this study numerical computations are carried out using 2000 layers, and, therefore in practice, a continuous fluid is analyzed. In fact, the description of the gyre remains based on layers of constant density, but when their number is large, both the thickness and the part directly exposed to the ventilation becomes very small for each layer,¹ and the density difference between nearest moving layers becomes negligible with respect to the density difference between thermocline bottom and abyss. This approach could produce a continuous model of the thermocline by taking the limit for the number of layers tending to infinity. The present study investigates the properties of the multilayer solution to gain some insight on how the thermocline interacts with the abyss.

In order to have the simplest dynamics, the presence of unventilated regions has been eliminated from the problem. Therefore, the theory developed in this paper is not complete because it cannot be applied to the fluid everywhere in the gyre, but it is valid only along the streamlines that outcrop, that is, reach the surface. Precisely, the theory is valid in the part the gyre where the whole column is ventilated. Its application to the whole basin requires the absence of the two regions called “shadow zone” and “unventilated pool” in the LPS theory, that is, the absence of streamlines departing from the lateral boundaries of the ocean. When the Ekman pumping velocity w_E , due to the wind stress, is negative, this condition is satisfied if the total depth of the thermocline vanishes both at the northern and eastern boundary and if the basin has no western boundary. It is, unfortunately, not easy to add a nonzero H at the eastern boundary. The method of solution of this paper does not easily generalize to the shadow zone that results in this case. However, the results of previous models, for example, the LPS model, show that in the region of the ventilated fluid the qualitative nature of the flow is unchanged. Moreover, The absence of limitation to the west eliminates the unventilated portion of the thermocline beneath the outcropping layers. Thus the region described by Young and Rhines (1982) is absent in the present model. We regard this as an unfortunate weakness of the present study but the simplification allows us to make considerable progress on the multilayer solution. Instead, we allow a finite density jump between the lowest ventilated stratum and the abyss, reminiscent of the solutions found by Salmon (1990) and Samelson and Vallis (1997) in which the unventilated domain shrinks to a narrow, near discontinuity in the absence of significant vertical diffusion. The method we employ differs from the approach of Huang (1988) in that we take as a starting point an analytical solution, described below, valid for an N -layer ventilated model, where N is arbitrary, and, in practice, very large.

The continuation of the paper consists of three sections. Section 2 presents the equations for generalizing the layer model to an arbitrary number of layers. Section 3 presents the properties of the solution and shows the results of its numerical computation for an idealized distribution of the surface density (assumed to be zonally constant and linearly increasing with latitude). Section 4 summarizes the outcome of the study.

2. Model with arbitrary number of layers

The thermocline is suspended over a quiescent abyss and is shielded from the direct action of the atmosphere by the surface mixed layer. The horizontal region occupied by the gyre is semi-infinite in the zonal direction (x coordinate) and is limited by the latitude circles corresponding to the values $f = 0$ and $f = f_{\max}$ of the Coriolis parameter f . The vertical structure of the thermocline is represented using $N + 1$ layers of constant density ρ_i , $\rho_i = \rho_0 + i\Delta\rho$, $i = 0, \dots, N$, where $\Delta\rho$ is a positive constant and ρ_0 is the density at the southern boundary of the gyre. The density range in the thermocline, $R = \rho_N - \rho_0$, is a fixed parameter in this study. The i th layer is delimited by the two surfaces $z_i(x, f)$ and $z_{i+1}(x, f)$, it has the thickness $h_i(x, f) = z_i(x, f) - z_{i+1}(x, f)$, and it outcrops along a line of constant latitude, which is denoted using the corresponding value of the Coriolis parameter \hat{f}_i (see Fig. 1). The lowermost moving level in the model is N and the total thickness of the thermocline is $H = -z_{N+1}(x, f)$. The density of the quiescent fluid below the thermocline is $\rho_A = \rho_N + \Gamma$ and,

as in general $\Gamma \neq 0$, even in the limit $\Delta\rho \rightarrow 0$ there is a discontinuity in the vertical profile of the density. The value of Γ is a parameter on which the solution of the problem depends and it represents the density difference between subpolar and midlatitude ocean. In the thermocline the motion is assumed frictionless, steady, adiabatic, hydrostatic, and geostrophic. The curl of the wind stress produces a negative Ekman pumping velocity with fluid passing from the mixed layer to the thermocline and forces the thermocline into motion.

Conceptually the model is the same that was described by [Luyten et al. \(1983\)](#) but it is extended here to an arbitrary number of layers. Since the motion is steady and adiabatic the transport in the i th layer,

$$(U_i(x, f), V_i(x, f)) = h_i(x, f)(u_i(x, f), \mathbf{v}_i(x, f)),$$

is nondivergent, except in the region where the layer is directly exposed to the pumping. Therefore a stream-function $\Psi_i(x, f)$ exists, such that

$$U_i(x, f) = -\beta \frac{\partial \Psi_i(x, f)}{\partial f}, \quad V_i(x, f) = \frac{\partial \Psi_i(x, f)}{\partial x}. \quad (1)$$

Since the motion is adiabatic and frictionless the potential vorticity is conserved for all layers except the uppermost one and since geostrophy holds,

$$\frac{D}{Dt} q_i(x, f) = \frac{D}{Dt} \frac{f}{h_i(x, f)} = 0, \quad (2)$$

which implies that $q_i(x, f)$ is constant along streamlines. Since the motion is steady and frictionless the Bernoulli function $b_i(x, f)$ is also constant along streamlines. In the linear approximation the Bernoulli function is $b_i(x, f) = p_i(x, f, z) + gz\rho_i$. Since the pressure is hydrostatic, it is given by the recursive relation:

$$p_A(x, f, z) = C - \rho_A g z, \quad (3)$$

$$p_N(x, f, z) = p_A(x, f, z) + \Gamma g(z - z_{N+1}(x, f)), \quad (4)$$

$$p_i(x, f, z) = p_{i+1}(x, f, z) + \Delta\rho g(z - z_{i+1}(x, f)), \quad (5)$$

where p_A is the pressure in the abyss and C is a constant. Consequently, the Bernoulli function is given by the relation:

$$b_A(x, f) = 0, \quad (6)$$

$$b_N(x, f) = -\Gamma g z_{N+1}(x, f), \quad (7)$$

$$b_i(x, f) = b_{i+1}(x, f) - \Delta\rho g z_{i+1}(x, f), \quad (8)$$

which can be rewritten

$$b_i(x, f) = -g \frac{R}{a} \left(z_{N+1}(x, f) + \frac{a}{N} \sum_{j=i+1}^N z_j(x, f) \right), \quad (9)$$

and where the parameter a

$$a = \frac{R}{\Gamma} \quad (10)$$

is introduced. Note that, unless $a \rightarrow \infty$, that is, Γ is zero, the lowermost layer of the thermocline is in motion. The crucial role of the parameter a will be explained in [section 3](#).

Since both $q_i(x, f)$ and $b_i(x, f)$ are constant along streamlines, then

$$q_i(x, f) = Q_i(b_i(x, f));(11)$$

that is, the potential vorticity is a function of $b_i(x, f)$, where the form of Q_i depends on the layer i . The total meridional transport V satisfies the Sverdrup relation

$$\beta V_S(x, f) = \beta \sum_{j=M}^N h_j(x, f) v_j(x, f) = f w_E(x, f), \quad (12)$$

valid for $f_M \leq f \leq f_{M+1}$ where M is the uppermost layer at the latitude f_M . The horizontal gradients of $b_i(x, f)$ and $p_i(x, f, z)$ coincide. Therefore, since the motion is geostrophic, $v_i(x, f)$ and $u_i(x, f)$ are given by

$$\begin{aligned} v_i(x, f) &= \frac{1}{\rho_* f} \frac{\partial b_i(x, f)}{\partial x}, \\ u_i(x, f) &= -\frac{\beta}{\rho_* f} \frac{\partial b_i(x, f)}{\partial f}, \end{aligned} \quad (13)$$

where ρ_* is the average density (the Boussinesq approximation is assumed). On the eastern boundary of the gyre the zonal velocity is required to vanish and therefore the levels $z_i(x, f)$ are constant (and, in this model, zero).

The method for solving the problem consists of two conceptual steps. The first step is to find the functions Q_i and to write Eq. (11) as a set of $N - M$ equations in the $N - M + 1$ variables $z_i(x, f)$, whose solution gives the levels $z_i(x, f)$ as a function of the lowermost level $z_{N+1}(x, f)$. The second step is to substitute this solution in the Sverdrup relation (12), using the geostrophic relation (13) for determining $z_{N+1}(x, f)$. At this point the Bernoulli function is known in each layer and the streamlines of the motion are determined.

a. The relation between potential vorticity and Bernoulli function

An interesting theoretical result and an iterative method for the solution of the ventilated thermocline problem are obtained by introducing a set of positive functions α_i , the fractional depth of the i th layer, defined as

$$z_i(x, f) = \alpha_i z_{N+1}(x, f). (14)$$

Each α_i varies between 0 and 1 ($\alpha_{N+1} \equiv 1$ is clearly a constant) and, a priori, could be a function of both the Coriolis parameter f and the x coordinate.

The derivation requires a few simple preliminary equations. Both potential vorticity and Bernoulli function are constant along streamlines after the fluid subducts, that is, for any x along a streamline in each layer i departing from the outcrop latitude \hat{f}_i at the longitude x' ,

$$q_i(x, f) = q_i(x', \hat{f}_i) \quad (15)$$

$$b_i(x, f) = b_i(x', \hat{f}_i). \quad (16)$$

Using the fractional thickness α_i , the expressions for the vorticity in the i th layer become

$$q_i(x, f) = \frac{f}{(\alpha_i(f) - \alpha_{i+1}(f))z_{N+1}(x, f)} \quad (17)$$

$$q_i(x', \hat{f}_i) = -\frac{\hat{f}_i}{\alpha_{i+1}(\hat{f}_i)z_{N+1}(x', \hat{f}_i)} \quad (18)$$

and the i th Bernoulli function, given by [Eq. \(9\)](#), is

$$b_i(x, f) = -g \frac{R}{a} z_{N+1}(x, f) \left(1 + \frac{a}{N} \sum_{j=i+1}^N \alpha_j(f) \right). \quad (19)$$

Note that the previous [Eqs. \(17\)–\(19\)](#) are valid also for $i = N$, with the convention that the sum gives no contribution for $i = N$.

Consider the N th layer. It is a matter of simple algebra to use sequentially the conservation of the potential vorticity along a streamline, [Eqs. \(15\)](#), [\(18\)](#), [\(19\)](#), and the conservation of the Bernoulli function along a streamline, [Eq. \(16\)](#), to obtain

$$q_N(x, f) b_N(x, f) = \hat{f}_N g \Gamma, \quad (20)$$

which shows that, in the N th layer, the Bernoulli function and the potential vorticity are inversely proportional. Moreover, using [Eq. \(17\)](#) and again [Eq. \(19\)](#) in the resulting [Eq. \(20\)](#), one obtains

$$\alpha_N \equiv \alpha_N(f) = 1 - \frac{f}{\hat{f}_N}, \quad (21)$$

which shows that the fractional thickness of the N th layer depends only on f .

If one assumes that the fractional thickness of layer $i + 1$ is known and that it is only a function of f , the reasoning carried out for the N th layer can be repeated for the i th layer. One obtains

$$q_i(x, f) b_i(x, f) = g \frac{R}{a} \frac{\hat{f}_i \left(1 + \frac{a}{N} \sum_{j=i+1}^N \alpha_j(\hat{f}_i) \right)}{\alpha_{i+1}(\hat{f}_i)}, \quad (22)$$

$$\alpha_i(f) = \alpha_{i+1}(f) - \alpha_{i+1}(\hat{f}_i) \frac{f}{\hat{f}_i} \frac{1 + \frac{a}{N} \sum_{j=i+1}^N \alpha_j(f)}{1 + \frac{a}{N} \sum_{j=i+1}^N \alpha_j(\hat{f}_i)}, \quad (23)$$

which shows that α_i does not depend on the x coordinate. [Equation \(23\)](#), valid in the region where layer i th is subducted, is a tool for the computations of the functions α_i from the bottom layer N to the uppermost subducted layer M . In other words, this basic conceptual step of our study provides us with an iterative procedure for the determination of the analytical expressions $\alpha_i(f)$ for $i = M, \dots, N$ and, consequently, of the corresponding levels $z_i(x, f)$ as functions of $z_{N+1}(x, f)$. We emphasize that the factors $\alpha_i(f)$ are functions only of f . They depend in a complicated way on the outcrop latitudes, but they do not depend on x .

Moreover, [Eqs. \(20\)](#) and [\(22\)](#) show that there is a set of positive constants, c_i , which are complicated functions of the outcrop latitudes,

$$c_N = g \frac{R}{a} \hat{f}_N, \quad (24)$$

$$c_i = g \frac{R}{a} \frac{\hat{f}_i \left(1 + \frac{a}{N} \sum_{j=i+1}^N \alpha_j(\hat{f}_i) \right)}{\alpha_{i+1}(\hat{f}_i)}, \quad (25)$$

such that

$$q_i(x, f)b_i(x, f) = c_i; (26)$$

that is, potential vorticity and Bernoulli function are inversely proportional with a coefficient that is known if the outcrop latitudes of the layers are known. Each coefficient c_i depends only on i , that is, the layer index ordering, and it is a function of $\hat{f}_j, j > i$. Thus, in general, the dependence of q_i on b_i is an inverse one, with the product $q_i b_i$ a function only of the density distribution at the sea surface.

Unfortunately the functions $\alpha_i(f)$ are expressed in terms of polynomials of degree $N - i + 1$, and consequently both their computations and the computation of c_i becomes analytically impractical if N is large. Note that α_N and α_{N-1} agree with the results of [Luyten et al. \(1983\)](#), in a region occupied by the directly ventilated fluid, when $N = 3$, and the density step between moving layers is constant.

b. The total depth of the thermocline

In order to solve the problem, after having found the constants $\alpha_i(f)$, one has to determine the total depth of the thermocline $z_{N+1}(x, f)$. Substituting in the Sverdrup relation [\(12\)](#), the geostrophic relation [\(13\)](#), and the [expressions \(9\)](#) and [\(14\)](#), after some algebra the relation

$$G_M(f) \frac{\partial}{\partial x} z_{N+1}^2(x, f) = w_E(x, f), \quad (27)$$

$$G_M(f) = \frac{R}{a} \frac{g\beta}{2\rho_* f^2} \sum_{i=M}^N (\alpha_{i+1}(f) - \alpha_i(f)) \times \left(1 + \frac{a}{N} \sum_{k=i+1}^N \alpha_k(f) \right) \quad (28)$$

is obtained, where $\alpha_{N+1}(f) \equiv 1$. The subscript M indicates that this expression is valid in the region where only the layers from M to N are present, that is, when the coriolis parameter varies from f_M to f_{M+1} . Having found $z_{N+1}(x, f)$ the streamlines for each layer can be determined using the [expressions \(9\)](#) and [\(14\)](#).

3. The analysis of the motion

The theory developed in this study allows the description of the motion in the thermocline using a very large number of layers and the analysis of the response of the thermocline structure to the magnitude of the density step at its bottom. This section is divided into two subsections. [Section 3a](#) analyzes the role of the density step at the bottom of the thermocline in term of the parameter $a = R/\Gamma$, and [section 3b](#) describes the method used for a numerical solution and shows the numerical solution for an idealized surface density distribution, constant in the zonal direction and linearly increasing with the latitude.

a. The dependence of the solution on the parameter a

The vertical structure of the thermocline depends on a , which controls both the baroclinicity and the nonlinearity of the problem. In fact, when the variation of the density in the thermocline, R , is negligible with respect to the step Γ at its bottom, the motion is conditioned only by the value of Γ and becomes barotropic. In the limit $a \rightarrow 0$, the nonlinear [equation \(23\)](#), which describes the fractional thickness of each layer $\alpha_i(f)$, becomes linear and its solution has the simple form $\alpha_i^{(0)}(f)$:

$$\alpha_i^{(0)}(f) = 1 - \frac{f}{\hat{f}_i}. \quad (29)$$

In this linear limit, the Bernoulli functions tend in every layer to the barotropic limit $b^{(0)}(x, f)$

$$b_i^{(0)}(x, f) = g \frac{R}{a} H(x, f), \quad (30)$$

and every function $G_i(f)$ has the same expression $G^{(0)}$:

$$G^{(0)}(f) = \frac{R}{a} \frac{g\beta}{2\rho_* f^2}. \quad (31)$$

The depth of the thermocline is given as the linear limit $H^{(0)}$:

$$H^{(0)}(x, f) = \left(\int_x^{x_E} \frac{w_E(x', f)}{G^{(0)}(f)} dx' \right)^{1/2}, \quad (32)$$

where $x \leq x_E$, eastern boundary of the gyre, and it reduces to that of the 1½ layer model. In this limit, the model is singular because as the thermocline depth tends to zero, the speed of every layer tends to infinity in order to maintain the prescribed Sverdrup transport.

The opposite limit is for $a \rightarrow \infty$, corresponding to $\Gamma \rightarrow 0$, that is, to the absence of discontinuity in the value of density at the bottom of the thermocline. This limit, where the motion is baroclinic and nonlinear, is called the “fully nonlinear” limit in this paper, and it represents the situation in which there is no density jump at the base of the ventilated thermocline. In this fully nonlinear limit, the most dense layer, whose Bernoulli function is given by

$$b_N(x, f) = g \frac{R}{a} H(x, f), \quad (33)$$

is not in motion, and the model is singular because the function $G_N(f)$, given by [Eq. \(28\)](#), tends to 0 and consequently the depth of the thermocline, given by [Eq. \(27\)](#), tends to infinity at its northern boundary. The singularity concerns the depth of the thermocline and not the fluid speed and the total transport. Precisely, the depth of the thermocline diverges as $a^{1/2}$, but the meridional fluid velocity $\mathbf{v}_N(x, f)$, given by [Eqs. \(13\)](#) and [\(33\)](#), tends to 0 as $a^{-1/2}$, and the meridional transport $V_N(x, f)$ is therefore finite.

The physical explanation is that the N th layer collects the infinite amount of fluid that flows at the sea surface along the semi-infinite northern boundary of the gyre, where the meridional velocity vanishes, and enters the gyre after having been ventilated for an infinite time. The flux of mass into the thermocline has to be balanced by a finite meridional transport, which, when there is no density difference between the bottom of the thermocline and the abyss and the fluid speed approaches smoothly the value of the abyss at rest, requires an infinite layer thickness. This represents a breakdown of the proposed model of the thermocline because the assumption of a vanishing thermocline depth at the northern boundary of the gyre cannot be maintained. The model is intrinsically inconsistent only in the fully nonlinear limit and a regular solution is possible when there is a finite step in both density and velocity at the bottom of the thermocline.

Actually, the continuous fluid, with a continuous vertical density distribution, is described by the fully nonlinear limit of this model, obtained for $N \rightarrow \infty$ and $\Gamma = \Delta\rho = (\rho_A - \rho_0)/(N + 1) \rightarrow 0$, and therefore $a \rightarrow \infty$. There is consequently a serious problem when this model is applied to the description of a continuous fluid and the density at the bottom of the thermocline approaches smoothly the density of the quiescent abyss, that is, if $\Gamma = \Delta\rho = (\rho_A - \rho_0)/(N + 1)$ tends to zero as N tends to infinity. Actually, the calculations of [Samelson and Vallis \(1997\)](#) suggest a value of Γ that is finite but different from 0. Therefore, the fully nonlinear limit of this model appears very interesting for the understanding of the motion of a continuous fluid, though it is not necessarily adequate for the description of the ocean thermocline.

Note that the lowermost N th layer has a peculiar behavior because its fractional thickness does not depend on a :

$$\alpha_N(f) = 1 - \frac{f}{\hat{f}_N} \quad \text{if } f < \hat{f}_N, \quad (34)$$

and moreover,

$$\begin{aligned}
h_N(x, f) &= \frac{f}{\hat{f}_N} H(x, f) \quad \text{if } f < \hat{f}_N, \\
h_N(x, f) &= H(x, f) \quad \text{if } f \geq \hat{f}_N,
\end{aligned} \tag{35}$$

which shows that, also in the limit $N \rightarrow \infty$ in which the thickness of every other layer tends to 0 and the multilayer fluid tends to a continuous one, the thickness of the N th layer remains finite, with a fractional value

$$\frac{z_N(x, f) - z_{N+1}(x, f)}{H(x, f)} = f/\hat{f}_N. \tag{36}$$

This means that the fluid in layer $N - 1$ is always a finite distance above the base of the thermocline, even though its outcrop line is infinitesimally close to the northern boundary of the gyre. This situation is a consequence of the idealized case that is analyzed in the paper, where the fluid in the N th layer has been ventilated at an infinite distance from the eastern boundary of the gyre. The fluid in the N th layer is forced to move along lines of constant thermocline depth H and also to conserve its potential vorticity. This fluid left the northern boundary of the gyre at an infinite distance from the eastern boundary, where the slope of the bottom of the thermocline was infinite in the meridional direction with a potential vorticity \hat{f}_N/H , and its thickness has to remain finite in order to conserve this finite vorticity at any latitude where $f \neq 0$. Note that the N th layer is the only layer whose potential vorticity, defined by [Eq. \(2\)](#), remains finite in the limit $N \rightarrow \infty$ when the vorticity of the other layers diverges, and that this behavior does not depend on the value of the Ekman pumping.

The value of a affects the fraction of total transport supported by each layer. In the linear limit, the motion is barotropic and the transport supported by each layer is proportional to the layer thickness. In this regime the lowermost N th layer, which occupies a large fraction of the thermocline thickness, gives the dominant contribution to the total transport. As a increases, the velocity of the fluid in the N th layer diminishes and its contribution to the total transport is reduced. Combining together the expression of the total Sverdrup transport [[Eq. \(12\)](#)] of the Bernoulli function in the N th layer [[Eq. \(7\)](#)] and of the thickness of the thermocline [[Eqs. \(27\)](#) and [\(28\)](#)], one obtains the ratio of the transport in the N th layer, $V_N(x, f) = \mathbf{u}_N(x, f)(z_N(x, f) - z_{N+1}(x, f))$ to the Sverdrup transport $V_S(x, f)$

$$\begin{aligned}
\frac{V_N(x, f)}{V_S(x, f)} &= \frac{f}{f_N} \left[\sum_{i=M}^N (\alpha_{i+1}(f) - \alpha_i(f)) \right. \\
&\quad \left. \times \left(1 + \frac{a}{N} \sum_{k=i+1}^N \alpha_k(f) \right) \right]^{-1}. \tag{37}
\end{aligned}$$

In the linear limit, the ratio is given by the ratio of the N th layer thickness to the total thickness, that is, f/f_N . In the fully nonlinear limit the ratio tends to 0, but at the northern boundary of the gyre. The vertical distribution of the transport has important consequences on the mass defect transport in each layer

$$\Phi_i(x, f) = \rho_i \mathbf{u}_i(x, f)(z_i(x, f) - z_{i+1}(x, f))$$

and on its total value $\Phi_M(x, f) = \sum_{i=M}^N \Phi_i$, where the subscript M indicates that this expression is valid in the region where only the layers from M to N are present, that is, when the Coriolis parameter varies from f_M to f_{M+1} . Since the lowermost layers transport the most dense fluid, a reduction of their volume transport implies a reduction of the total mass transport in the thermocline.

b. The numerical solution

The derivation of an analytical expression for the fractional layer thickness $\alpha_i(f)$ using [Eq. \(23\)](#) and starting from layer N is possible in principle, but, as the layer index decreases, the resulting expressions are increasingly complicated and practically useless. Consequently, the analytical solution is useful for the understanding of the thermocline dynamics only when the number of layers is very small. On the other hand, the numerical solution can be easily derived from [Eqs. \(23\)](#) and

(27), and also when the number of layers N is very large, by describing the horizontal domain with N_j steps in the meridional direction and N_k steps in the zonal direction.

The discrete version of Eq. (23) is easily obtained:

$$\alpha_{i,j} = \alpha_{i+1,j} - \frac{f_j^*}{\hat{f}_i^*} \alpha_{i+1,l_i} \frac{1 + \frac{a}{N} \sum_{k=i+1}^N \alpha_{k,j}}{1 + \frac{a}{N} \sum_{k=i+1}^N \alpha_{k,l_i}}, \quad (38)$$

where $f_j^* = j/N_j$, $j = 1, \dots, N_j$ is the dimensionless Coriolis parameter, $\alpha_{i,j} = \alpha_i(f_j^*)$, and l_i denotes the index corresponding to the outcrop line of layer i , that is, $f_{l_i} = \hat{f}_i$. Because of the definition (14) one has $\alpha_{N+1,j} = 1$, for $j = 0, \dots, N_j$, and north of the outcrop line of layer i , that is, for $j \geq l_i$, $\alpha_{i,j} = 0$. In the region $j < l_i$ the variables $\alpha_{i,j}$ are determined using (38).

Assuming that the Ekman pumping velocity depends only on latitude, the equation for the total dimensionless depth of the thermocline is

$$H_{k,j}^* = \frac{g\beta R}{W_E L 2\rho_* \hat{f}_N} H_{k,j}, \quad k = 1, \dots, N_k, \\ j = 1, \dots, N_j, \quad (39)$$

where the first index k denotes the dimensionless distance from the eastern boundary of the gyre $x_k^* = k/N_k$, the second index j denotes the meridional coordinate, W_E represents the magnitude of the Ekman pumping velocity; L , the zonal extension of the domain of integration, is

$$H_{k,j}^* = \left(\frac{w_{Ej}^*(x_k^* - 1)}{G_j^*} \right)^{1/2}. \quad (40)$$

Here w_{Ej} is the dimensionless Ekman pumping velocity, and

$$G_j^* = \frac{1}{af_j^{*2}} \left[f_j^* + \sum_{i=j}^N (\alpha_{j+1,i} - \alpha_{i,j}) \left(1 + \frac{a}{N} \sum_{k=i+1}^N \alpha_{k,j} \right) \right]. \quad (41)$$

The dimensionless level z_{ijk}^* of the i th layer at the distance $x_k^* = k/N_k$ from the eastern boundary of the gyre and at the latitude $f_j^* = j/N_j$ is determined as

$$z_{ijk}^* = -\alpha_{i,j} H_{k,j}^*, \quad (42)$$

and the Bernoulli function for the same layer at the same point is

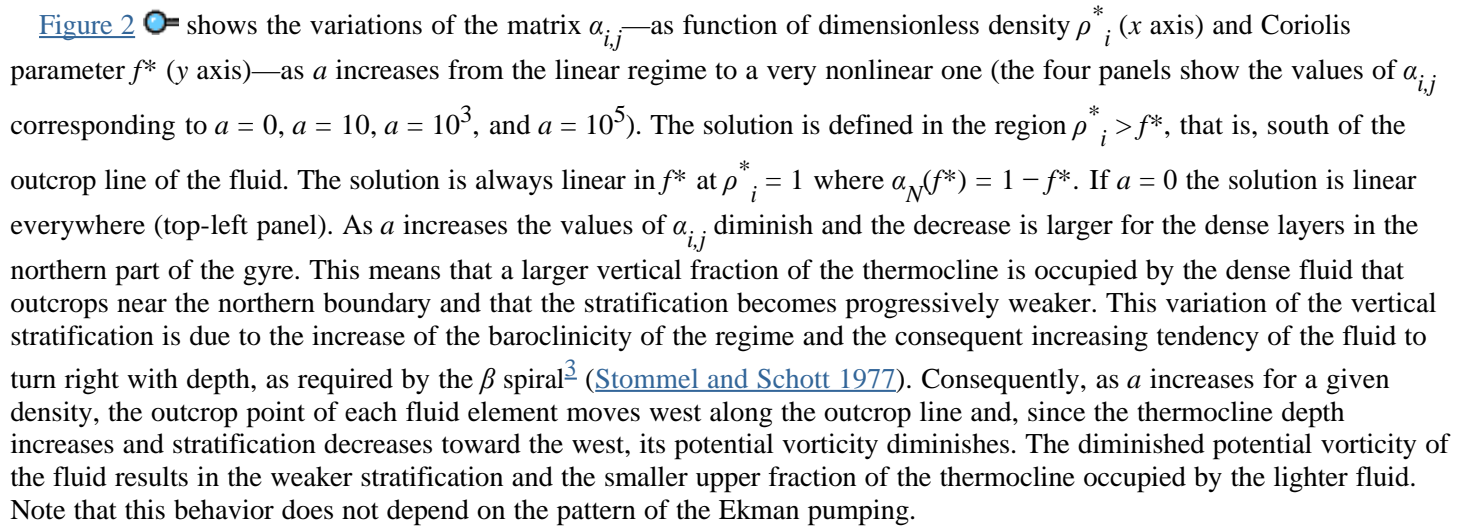
$$b_{i,j,k}^* = \frac{z_{N+1,j,k}^*}{a} \left(1 + \frac{a}{N} \sum_{m=i+1}^N \alpha_{m,j} \right). \quad (43)$$

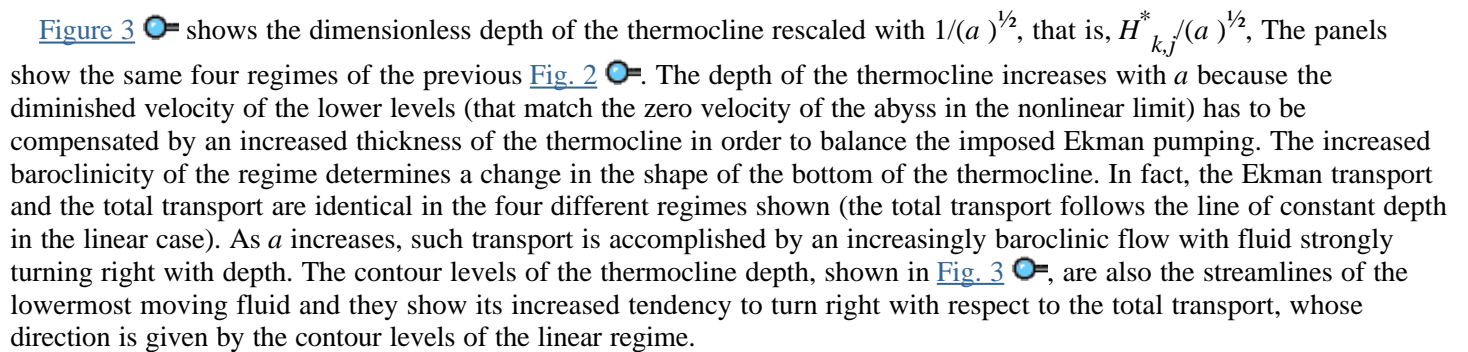
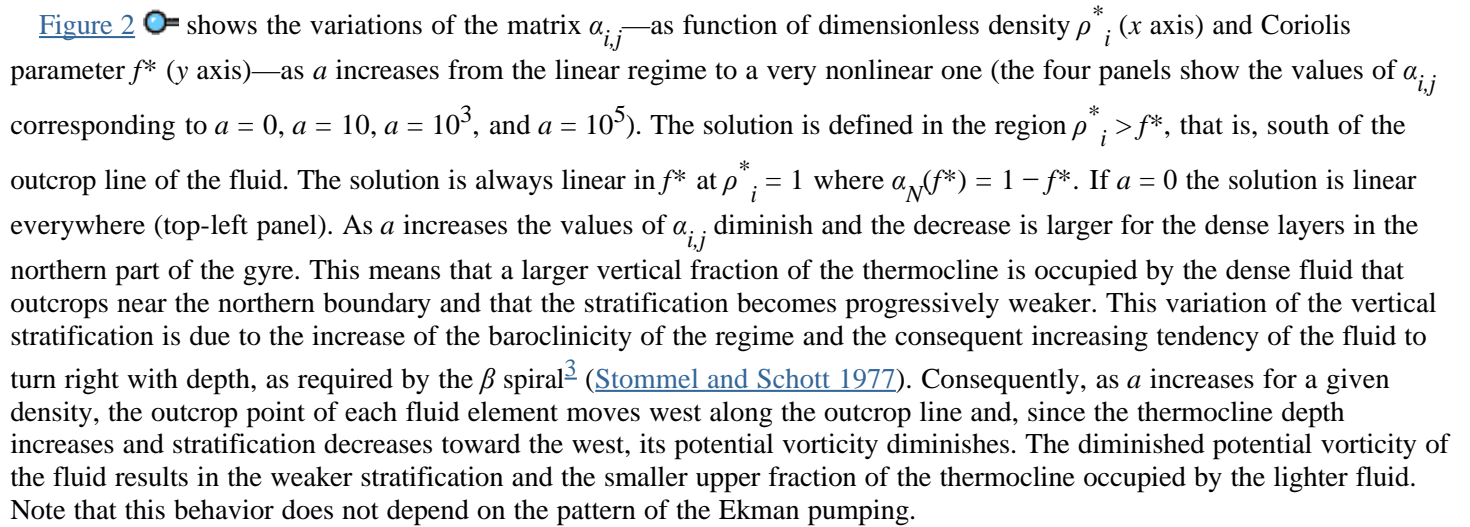
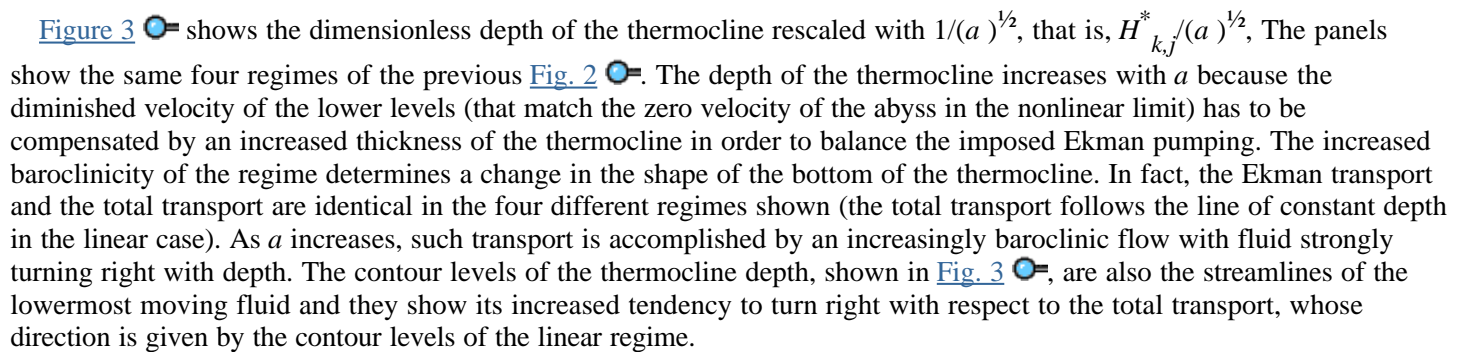
Figures 2–7 show the results of the numerical computation, specifying

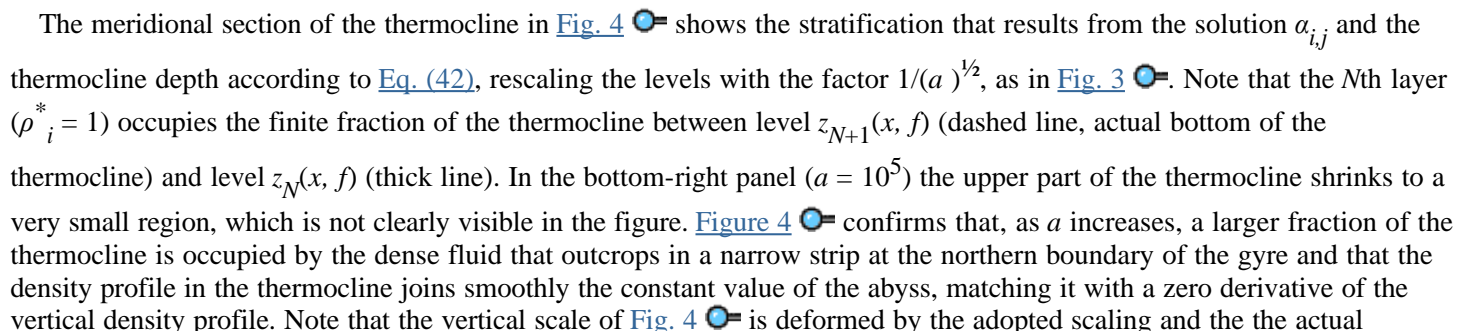
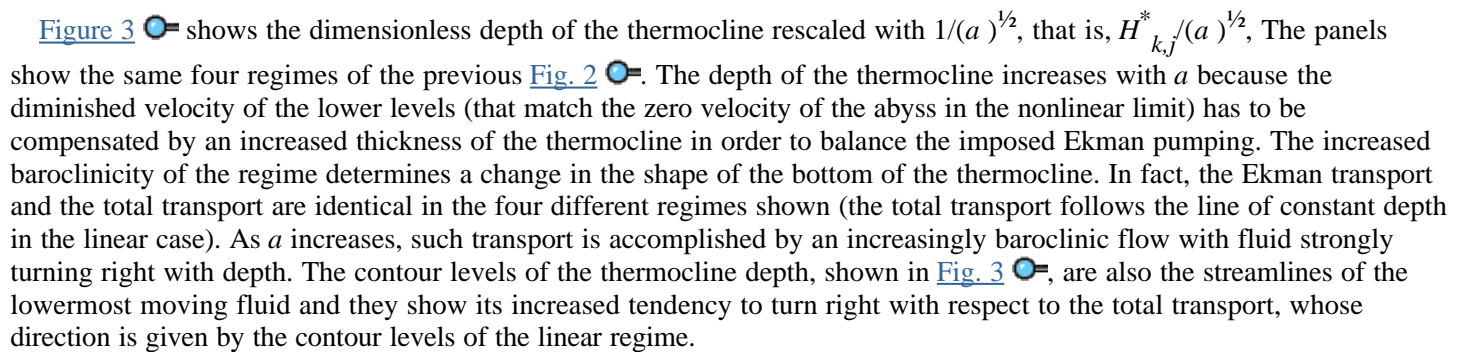
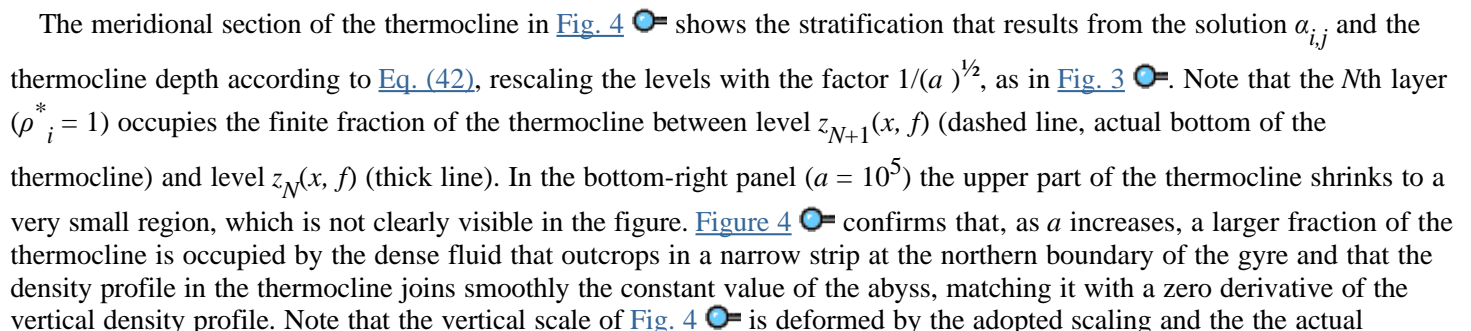
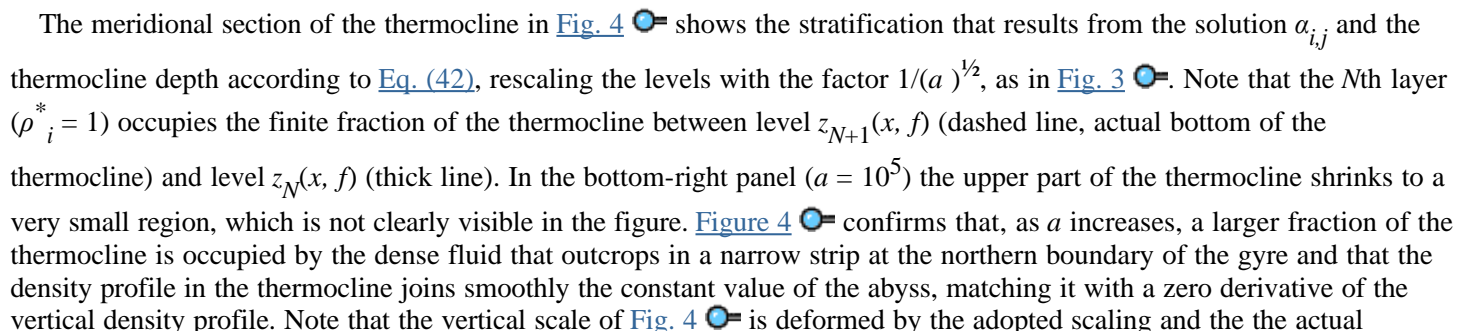
$$w_{Ej}^* = -\sin\left(\pi \frac{j}{N_j}\right), \quad (44)$$

and imposing a constant linear gradient of the surface density along the whole meridional extension of the gyre, such that $\rho = \rho_N$ at the northern boundary and $\rho = \rho_0$ at the southern boundary. The outcrop line is given by the relation $\hat{f}_i = \rho_i^*$ with $\rho_i^* = (\rho_i - \rho_0)/(\rho_N - \rho_0)$.


In the actual computation the density step was not constant, but a fine $\Delta\rho$ has been used near the northern boundary of the gyre in order to resolve adequately the details of the nonlinear flow. In fact, the solution was computed with the requirement that the density jump at the base of the thermocline was much larger than the density resolution within the thermocline; that is, $\Gamma \gg \Delta\rho$, which requires $a \ll N$. This ensures that the “1” in [Eq. \(23\)](#) is never negligible and the solution has a smooth transition from the linear to the nonlinear regime. The whole range of density was split into two intervals. From $\rho_i^* = 0$ to $\rho_i^* = 1 - 1/N_c$, the equation was integrated using a coarse step $\Delta\rho = 1/N_c$, while from $1 - 1/N_c$ to 1 the equation was integrated using a fine step $\Delta\rho = 1/N_f$. Note that this implies some trivial changes in the formulas.² The solution shown was obtained using $N_c = 2 \cdot 10^3$ layers, and $N_f = 2 \times 10^7$ if $a = 10^5$, $N_f = 4 \times 10^6$ in the other cases. In the meridional direction $N_j = N_c$ and $N_j = N_f$ latitudes were used in the coarse resolution and fine resolution range, respectively. $N_k = 100$ longitudes were used in the zonal direction.


[Figure 2](#)  shows the variations of the matrix $\alpha_{i,j}$ —as function of dimensionless density ρ_i^* (x axis) and Coriolis parameter f^* (y axis)—as a increases from the linear regime to a very nonlinear one (the four panels show the values of $\alpha_{i,j}$ corresponding to $a = 0$, $a = 10$, $a = 10^3$, and $a = 10^5$). The solution is defined in the region $\rho_i^* > f^*$, that is, south of the outcrop line of the fluid. The solution is always linear in f^* at $\rho_i^* = 1$ where $\alpha_N(f^*) = 1 - f^*$. If $a = 0$ the solution is linear everywhere (top-left panel). As a increases the values of $\alpha_{i,j}$ diminish and the decrease is larger for the dense layers in the northern part of the gyre. This means that a larger vertical fraction of the thermocline is occupied by the dense fluid that outcrops near the northern boundary and that the stratification becomes progressively weaker. This variation of the vertical stratification is due to the increase of the baroclinicity of the regime and the consequent increasing tendency of the fluid to turn right with depth, as required by the β spiral³ ([Stommel and Schott 1977](#)). Consequently, as a increases for a given density, the outcrop point of each fluid element moves west along the outcrop line and, since the thermocline depth increases and stratification decreases toward the west, its potential vorticity diminishes. The diminished potential vorticity of the fluid results in the weaker stratification and the smaller upper fraction of the thermocline occupied by the lighter fluid. Note that this behavior does not depend on the pattern of the Ekman pumping.

[Figure 3](#)  shows the dimensionless depth of the thermocline rescaled with $1/(a)^{1/2}$, that is, $H_{k,j}^*/(a)^{1/2}$. The panels show the same four regimes of the previous [Fig. 2](#) . The depth of the thermocline increases with a because the diminished velocity of the lower levels (that match the zero velocity of the abyss in the nonlinear limit) has to be compensated by an increased thickness of the thermocline in order to balance the imposed Ekman pumping. The increased baroclinicity of the regime determines a change in the shape of the bottom of the thermocline. In fact, the Ekman transport and the total transport are identical in the four different regimes shown (the total transport follows the line of constant depth in the linear case). As a increases, such transport is accomplished by an increasingly baroclinic flow with fluid strongly turning right with depth. The contour levels of the thermocline depth, shown in [Fig. 3](#) , are also the streamlines of the lowermost moving fluid and they show its increased tendency to turn right with respect to the total transport, whose direction is given by the contour levels of the linear regime.


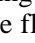
The meridional section of the thermocline in [Fig. 4](#)  shows the stratification that results from the solution $\alpha_{i,j}$ and the thermocline depth according to [Eq. \(42\)](#), rescaling the levels with the factor $1/(a)^{1/2}$, as in [Fig. 3](#) . Note that the N th layer ($\rho_i^* = 1$) occupies the finite fraction of the thermocline between level $z_{N+1}(x, f)$ (dashed line, actual bottom of the thermocline) and level $z_N(x, f)$ (thick line). In the bottom-right panel ($a = 10^5$) the upper part of the thermocline shrinks to a very small region, which is not clearly visible in the figure. [Figure 4](#)  confirms that, as a increases, a larger fraction of the thermocline is occupied by the dense fluid that outcrops in a narrow strip at the northern boundary of the gyre and that the density profile in the thermocline joins smoothly the constant value of the abyss, matching it with a zero derivative of the vertical density profile. Note that the vertical scale of [Fig. 4](#)  is deformed by the adopted scaling and the the actual

dimensionless thickness of the thermocline increases almost as $(a)^{1/2}$.

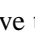
[Figure 5](#)  shows the streamline of the flow for three selected levels and the transition from the linear and barotropic to the nonlinear and baroclinic regime. The density levels are chosen in order to describe the region of stronger baroclinicity, that is, the lower part of the thermocline. The lowermost level shown is immediately above the bottom of the thermocline ($\rho_i^* = 0.99$). The two other levels shown are $\rho_i^* = 0.9$ and $\rho_i^* = 0.5$. In the linear case the motion is fully barotropic. As a increases, the streamlines turn right with depth and the point where they reach the outcrop line moves toward the west. This effect is larger for the deeper fluid, represented by the layers $\rho_i^* = 0.9$ and $\rho_i^* = 0.99$, while the effect on the layer $\rho_i^* = 0.5$ and the upper part of the thermocline is small.

[Figure 6](#)  shows the dimensionless meridional volume transport for the same four regimes. The lowermost dashed line represents the total dimensionless Sverdrup transport, $V_S^* = f^* w_E^*$, which obviously does not depend on a . The dimensionless transport of the i th layer is defined as

$$V_i^* = [v_i(z_i(x, f) - z_{i+1}(x, f))] \frac{f^* w_E^*}{f w_E}. \quad (45)$$

The density range has been divided into 10 intervals. The thin continuous lines represent the cumulated transport up to density $\rho_i^* = 0.1n$, $n = 1, \dots, 9$. The lowermost continuous thick line represents the cumulated contribution up to layer $N - 1$. [Figure 6](#)  shows that the contribution of the N th layer, given by the space between dashed and thick lines, diminishes for increasing a , and its share is taken over by the lighter layers above it. This is a consequence of the progressively lower speed of the fluid near the base of the thermocline for increasing a . [Figure 7](#)  shows the dimensionless mass defect transport. The dimensionless mass defect transport of the i th layer is defined as

$$\Phi_i^* = (\rho_0^* - \rho_i^*) V_i^*. \quad (46)$$

Lines have the same meaning as in [Fig. 6](#) ; that is, the cumulated mass transport Φ^* is shown. Since, as a increases, the speed of the lowest layers diminishes, the amount of most dense fluid flowing toward the equator decreases and the overall mass transport is reduced. The reduction, not very large, is approximately 10% in the middle of the gyre at $f^* = 0.5$. Since the high density of the fluid is generally due to its low temperature, the diminished mass transport is associated with a diminished meridional heat transport.

4. Conclusions

The main results of this study are [Eqs. \(23\)–\(28\)](#). They provide the tools for the description of the flow in the ventilated part of the thermocline. The basic equation is actually [Eq. \(26\)](#), showing that potential vorticity and Bernoulli function are inversely proportional, and that their product, the constants c_i , depends only on the surface density distribution. The constants c_i characterize the whole problem, and their knowledge would make it linear. In continuation of the research it will be interesting to search for a family of expressions of c_i depending on a convenient parameter and corresponding to a reasonable distribution of the surface density, such that an analytical tractable solution of [Eq. \(23\)](#) exists. The analysis of the behavior of the solution as the parameter varies could give interesting information on the dynamics of the thermocline.

We have limited our attention for simplicity to the case of zonal outcrop lines, as we have already mentioned, for simplicity. We realize that for other outcrop line configurations the relationship that we derived between the potential vorticity and the Bernoulli function will differ. Indeed, as [Williams \(1991\)](#) shows (see also [Pedlosky 1996](#)), it is possible that variable mixed layer thickness, or differently configured outcrop geometries, can lead to even uniform potential vorticity for the ventilated fluid. Anyway, since the zonal outcrop case is in some sense the classical statement of the problem and since the outcrops in the ocean approximate zonality, it is a case of particular interest.

The numerical solution describes the mapping of the density distribution from the surface to the vertical thickness of the gyre. The relative importance of the surface density contrast $\rho_N - \rho_0$, where ρ_N, ρ_0 are the maximum and minimum density in the thermocline, respectively, versus the density step Γ between bottom of the thermocline and the abyss is found to be the parameter that controls the behavior of the solution. The dependence of the solution on this parameter

$$a = \frac{\rho_N - \rho_0}{\Gamma}$$

has been investigated. When $a = 0$, the solution is barotropic and the basic Eq. (23) is linear. The motion becomes progressively more baroclinic and Eq. (23) more nonlinear as a increases. It is shown that the depth of the thermocline increases with a . Moreover, as the nonlinearity increases, the vertical stratification decreases, fluid of progressively lower potential vorticity fills the lower part of the thermocline, and the total thickness of the thermocline becomes larger. Though the total volume transport does not depend on the value of a , the transport supported by each layer varies with a . When a is not large, say, between 0 and 10, most of the transport is mainly supported by the most dense layer N , whose share, for increasing a , is taken over by the less dense fluid and vanishes for a tending to infinity. This dependence of the distribution of the volume transport among different layers influences the mass transport because it affects the amount of most dense fluid flowing southward. Consequently, when a increases, the mass transport diminishes. The computed reduction, when a varies from 0 to 10^5 , is approximately 10%. Since the surface variation of density is associated with a variation of temperature, the diminished mass transport is associated with a diminished heat transport. According to this model the diminished temperature difference between midlatitudes and the subpolar ocean corresponds to a diminished heat transport in the thermocline from the midlatitudes to the equator, which, acting as a positive feedback, might further diminish the temperature difference between subpolar and midlatitude ocean. This stresses the importance of the interaction between thermocline and abyss for the determination of the motion within the thermocline.

If Γ is nonzero, as suggested by other calculations (Samelson and Vallis 1997), the solution is finite, and moreover, it can be shown that the limit of large N goes smoothly to the continuous limit (we are in the process of preparing a paper describing our results). Our model fails in the limit $a \rightarrow \infty$ because it predicts an infinite thermocline depth. This singularity derives from the need for balancing the volume mass due to the Ekman pumping at the northern boundary of the gyre in the special situation when the most dense layer matches the density of the abyss ($\Gamma \rightarrow 0$), and therefore its speed becomes vanishingly small. Since the required meridional transport is finite, an infinite layer thickness results.

The extension of our results to the continuous ocean, without the discontinuity in density at the bottom of the thermocline, presents some interesting problems. Such a continuous limit can be obtained by assuming $\Gamma = \Delta\rho \rightarrow 0$ as $N \rightarrow \infty$, and therefore $a \rightarrow \infty$. This shows that this model is singular in the continuous limit. This singularity is probably due to both the model dynamics and the idealized basin geometry. The model dynamics is lacking because there is no mechanism capable of setting into motion the underlying, more dense layers that are not directly exposed to the ventilation. The introduction of a western boundary of the gyre should limit the fluid pushed by the Ekman pumping inside the ocean at the northern boundary and possibly eliminate the singularity in the thermocline depth. It would be of considerable interest to see whether the present solution, based on the general iterative solution for layer depth given by Eq. (23), could be extended to include the presence of unventilated homogenized regions beneath the ventilated zone. Note that the assumed vanishing thickness of the ventilated fluid at the northern boundary of the gyre cannot be considered a limitation of the model, but it reflects the presence in the real ocean of ventilated fluid that outcrops at the northern boundary of the gyre. The unrealistic model feature is not the presence of such a layer, but the absence of a dynamics capable of setting into motion the underlying unventilated portion of the thermocline.

In conclusion, the model is clearly incomplete in that it ignores the motion of the unventilated fluid that would outcrop in the subpolar gyre. Although such a restriction is dynamically consistent, the work of Young and Rhines (1982) has shown the likelihood of the instability of such solutions with respect to solutions in which the total Sverdrup transport is shared with the deeper unventilated strata on which q is homogenized in pools nestled against the northwestern corner of the basin. The solution we have presented may therefore have relevance only in the eastern portion of the basin where the Young–Rhines layer is extremely thin. We find it suggestive that our solution indicates that the stratification in the deepest ventilated part of the thermocline should be substantially weaker than in the upper one. That aspect of the solution recurs in the more realistic model of Samelson and Vallis (1997), especially when the vertical diffusivity is small and the base of the ventilated thermocline is separated from the nearly uniform abyss by a region of extremely sharp density gradient, which in our model we associate with a density jump at the base of the ventilated thermocline. Such regions of “mode” water may be a natural product of the process of wind-driven surface ventilation. Although the model is highly idealized and ignores the motion of unventilated water beneath the thermocline, it has allowed us to obtain some important insights into the thermocline structure. Thus the inverse relation between potential vorticity q and Bernoulli function b described by Eq. (26) has been proved, the dependence of the motion in the thermocline on the difference in density between thermocline bottom and abyss has been investigated, and the singularity of a model whose dynamics completely neglects diffusive processes in a zonally semi-infinite basin with a continuous vertical density profile has been found.

REFERENCES

- Huang, R. X., 1988: On boundary value problems of the ideal-fluid thermocline. *J. Phys. Oceanogr.*, **18**, 619–641. [Find this article online](#)
- Luyten, J. R., J. Pedlosky, and H. Stommel, 1983: The ventilated thermocline. *J. Phys. Oceanogr.*, **13**, 292–309. [Find this article online](#)
- McCartney, M. S., and L. D. Talley, 1984: Warm-to-cold conversion in the North Atlantic Ocean. *J. Phys. Oceanogr.*, **14**, 922–935. [Find](#)

Pedlosky, J., 1996: *Ocean Circulation Theory* (Chapter 4), Springer-Verlag, 453 pp..

Salmon, R., 1990: The thermocline as an “internal boundary layer.” *J. Mar. Res.*, **48**, 437–469..

Samelson, R. M., and G. K. Vallis, 1997: Large scale circulation with small diapycnal diffusion: The two thermocline limit. *J. Mar. Res.*, in press..

Schmitz, W. J., J. D. Thompson, and J. R. Luyten, 1992: The Sverdrup circulation for the Atlantic along 24°N. *J. Geophys. Res.*, **97**, 7251–7256..

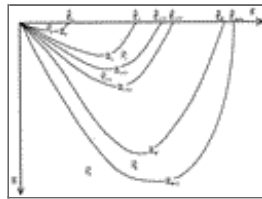
Semtner, A. J., and R. M. Chervin, 1988: A simulation of the global ocean circulation with resolved eddies. *J. Geophys. Res.*, **93**, 15 502–15 522..

Stommel, H., and F. Schott, 1977: The beta spiral and the determination of the absolute velocity field from hydrographic data. *Deep-Sea Res.*, **24**, 325–329..

Williams, R. G., 1991: The role of the mixed layer in setting the potential vorticity of the main thermocline. *J. Phys. Oceanogr.*, **21**, 1803–1814.. [Find this article online](#)

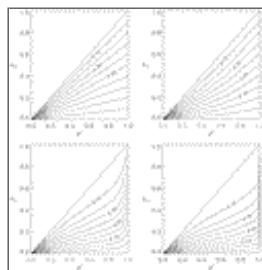
Young, W. R., and P. B. Rhines, 1982: A theory of the wind-driven circulation. II. Gyres with western boundary layers. *J. Mar. Res.*, **40**, 849–872..

Figures



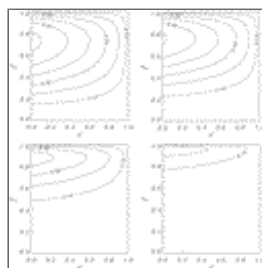
[Click on thumbnail for full-sized image.](#)

Fig. 1. Schematic of the layer model: meridional section of the gyre.



[Click on thumbnail for full-sized image.](#)

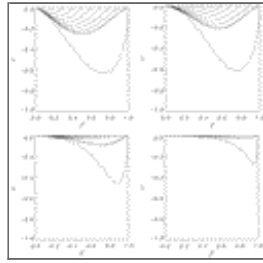
Fig. 2. The solution $\alpha_{i,j}$ as function of ρ^* (x axis) and f^* (y axis) for increasing value of the parameter a . Top-left: linear case, top-right: $a = 10$, bottom-left: $a = 10^3$, and bottom-right: $a = 10^5$.



[Click on thumbnail for full-sized image.](#)

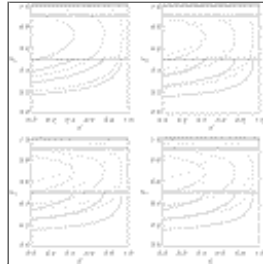
Fig. 3. Dimensionless level of the bottom of the thermocline H^* rescaled with $a^{-1/2}$ as a function of dimensionless distance from the eastern boundary x^* (x axis) and of the Coriolis parameter f^* (y axis). Top-left: linear case, top-right: $a = 10$, bottom-left: $a = 10^3$, and bottom-right: $a = 10^5$.

$= 10^3$, and bottom-right: $a = 10^5$.



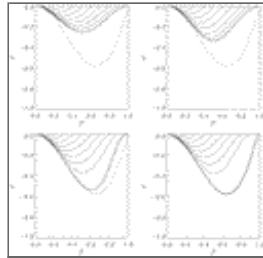
[Click on thumbnail for full-sized image.](#)

Fig. 4. Meridional section of the stratification. The dimensionless z^* levels rescaled with $a^{-1/2}$ are plotted as function of f^* . The lowermost dashed line is the dimensionless bottom of the thermocline, $-H^*(1, f^*)$. The thick line is $z^*(1 - 1/N, 1, f^*)$. The remaining lines are $z^*(0.9, 1, f^*)$ to $z^*(0.1, 1, f^*)$ with a step $\Delta\rho^* = 0.1$ Top-left: linear case, top-right: $a = 10$, bottom-left: $a = 10^3$, and bottom-right: $a = 10^5$.



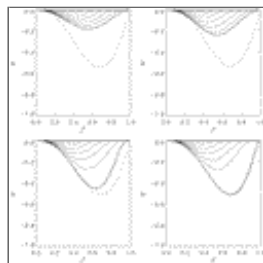
[Click on thumbnail for full-sized image.](#)

Fig. 5. Streamlines of the flow. The dotted lines show $b^*(0.99, x^*, f^*)$, the dashed lines show $b^*(0.9, x^*, f^*)$, and the continuous lines show $b^*(0.5, x^*, f^*)$. The thick lines evidence the outcrop latitudes of layer $\rho_{i*} = 0.99, \rho_{i*} = 0.9$, and $\rho_{i*} = 0.5$. Top-left: linear case (note that the motion is barotropic), top-right: $a = 10$, bottom-left: $a = 10^3$, and bottom-right: $a = 10^5$ case.



[Click on thumbnail for full-sized image.](#)

Fig. 6. Dimensionless volume transports, V^* , as functions of f^* . The lowermost dashed line is the dimensionless total Sverdrup transport. The thin lines show the cumulated transports up to layer $\rho^* = n^* \Delta\rho^*$, $n = 1, \dots, 9$, $\Delta\rho^* = 0.1$, The thick line, the transport up to layer $\rho^* = 1 - 1/N$. Top-left: linear case, top-right: $a = 10$, bottom-left: $a = 10^3$, and bottom-right: $a = 10^5$.



[Click on thumbnail for full-sized image.](#)

Fig. 7. Dimensionless mass transports, Φ^* , as functions of f^* . The lowermost dashed line is the total transport. The thin lines show the cumulated transports up to layer $\rho^* = n^* \Delta\rho^*$, $n = 1, \dots, 9$, $\Delta\rho^* = 0.1$, The thick line, the transport up to layer $\rho^* = 1 - 1/N$. Top-left: linear case, top-right: $a = 10$, bottom-left: $a = 10^3$, and bottom-right: $a = 10^5$.

¹ Actually the thickness of the lowermost layer remains finite. This is explained in [section 3a](#).

² When two different density steps are used, the factor $1/N$ is eliminated from the sums in [Eq. \(38\)](#) and each layer is given a weight proportional to the density step, that is, $\Delta\rho = 1/N_f$ in the fine resolution range and $\Delta\rho = 1/N_c$ in the coarse resolution range. This change is obvious if one considers the sums as the discrete representation of integrals in density.

³ This is confirmed by the analysis of the streamlines discussed later in this section.

Corresponding author address: Dr. Piero Lionello, Department of Physics, University of Padua, via Marzolo 8, 35131 Padua, Italy.

E-mail: piero.lionello@pd.infn.it

top ▲



© 2008 American Meteorological Society [Privacy Policy and Disclaimer](#)

Headquarters: 45 Beacon Street Boston, MA 02108-3693

DC Office: 1120 G Street, NW, Suite 800 Washington DC, 20005-3826

amsinfo@ametsoc.org Phone: 617-227-2425 Fax: 617-742-8718

[Allen Press, Inc.](#) assists in the online publication of *AMS* journals.